

The Short-period S-stars S4711, S62, S4714 and the Lense–Thirring Effect due to the Spin of Sgr A^{*}

Lorenzo Iorio¹

Ministero dell’Istruzione, dell’Università e della Ricerca (M.I.U.R.)

Viale Unità di Italia 68, I-70125, Bari (BA), Italy

`lorenzo.iorio@libero.it`

Received _____; accepted _____

Abstract

Recently, some S-stars (S4711, S62, S4714) orbiting the supermassive black hole (SMBH) in Sgr A* with short orbital periods ($7.6 \text{ yr} \leq P_b \leq 12 \text{ yr}$) were discovered. It was suggested that they may be used to measure the general relativistic Lense-Thirring (LT) precessions of their longitudes of ascending node Ω induced by the SMBH's angular momentum \mathbf{J}_\bullet . In fact, the proposed numerical estimates hold only in the particular case of a perfect alignment of \mathbf{J}_\bullet with the line of sight, which does not seem to be the case. Moreover, also the inclination I and the argument of perinigricon ω also undergo LT precessions for an arbitrary orientation of \mathbf{J}_\bullet in space. We explicitly show the analytical expressions of \dot{I}^{LT} , $\dot{\Omega}^{\text{LT}}$, $\dot{\omega}^{\text{LT}}$ in terms of the SMBH's spin polar angles i^\bullet , ε^\bullet . It turns out that the LT precessions, in arcseconds per year ($'' \text{ yr}^{-1}$), range within $|\dot{I}^{\text{LT}}| \lesssim 7'' \text{ yr}^{-1}$, $|\dot{\Omega}^{\text{LT}}| \lesssim 9'' \text{ yr}^{-1}$, and $-13'' \text{ yr}^{-1} \lesssim \dot{\omega}^{\text{LT}} \lesssim 14'' \text{ yr}^{-1}$ for S4714, $|\dot{I}^{\text{LT}}| \lesssim 5'' \text{ yr}^{-1}$, $|\dot{\Omega}^{\text{LT}}| \lesssim 5'' \text{ yr}^{-1}$, and $|\dot{\omega}^{\text{LT}}| \lesssim 10'' \text{ yr}^{-1}$ for S62, and $|\dot{I}^{\text{LT}}| \lesssim 0.3'' \text{ yr}^{-1}$, $|\dot{\Omega}^{\text{LT}}| \lesssim 0.3'' \text{ yr}^{-1}$, and $|\dot{\omega}^{\text{LT}}| \lesssim 0.7'' \text{ yr}^{-1}$ for S4711. For each star, the corresponding values of i_{max}^\bullet , $\varepsilon_{\text{max}}^\bullet$, and i_{min}^\bullet , $\varepsilon_{\text{min}}^\bullet$ are determined as well, along with those i_0^\bullet , ε_0^\bullet that cancel the LT precessions. The LT perinigricon precessions $\dot{\omega}^{\text{LT}}$ are overwhelmed by the systematic uncertainties in the Schwarzschild ones due to the current errors in the stars' orbital parameters and the mass of Sgr A* itself.

keywords Kerr black holes (886); Orbital elements (1177); General relativity (641);

1. Introduction

Recently, Peißker et al. (2020) discovered some main sequence stars revolving around the supermassive black hole (SMBH) allegedly lurking in the Galactic Center (GC) at Sgr A* (Ghez et al. 2008; Genzel, Eisenhauer & Gillessen 2010) characterized by very high eccentricities and relatively short orbital periods P_b with respect to the star S2 (Martins et al. 2008) ($P_b = 16 \text{ yr}$) and other S-stars (Gillessen et al. 2017); they are listed in Table 1. Gravity Collaboration et al. (2020) were able to successfully measure the general relativistic Schwarzschild-like precession of the perinigricon ω

$$\dot{\omega}^{\text{Sch}} = \frac{3 n_b \mu}{c^2 a (1 - e^2)} \quad (1)$$

of S2 with a 19% accuracy; in Equation (1), c is the speed of light in vacuum, a is the semimajor axis, e is the eccentricity, $n_b = 2\pi/P_b$, and $\mu \doteq GM$ is the primary's gravitational parameter given by the product of its mass M and the Newtonian gravitational constant G . Previously, the combined gravitational redshift and relativistic transverse Doppler effect of S2 were detected by Gravity Collaboration et al. (2018) with a $\simeq 15\%$ accuracy. All such gravitational effects,¹ due to

¹The transverse Doppler shift is predicted by the special theory of relativity.

Table 1: Relevant Orbital Parameters of Some Selected Short-period S-stars Retrieved from Table 2 of Peißker et al. (2020).

Star	a (mpc)	P_b (yr)	e	I (°)	Ω (°)
S4714	4.079 ± 0.012	12.0 ± 0.3	0.985 ± 0.011	127.70 ± 0.28	129.28 ± 0.63
S62	3.588 ± 0.02	9.9 ± 0.3	0.976 ± 0.01	72.76 ± 5.15	122.61 ± 4.01
S4711	3.002 ± 0.06	7.6 ± 0.3	0.768 ± 0.030	114.71 ± 2.92	20.10 ± 3.72

Note. Here, a is the semimajor axis, in milliparsecs (mpc), $P_b = 2\pi \sqrt{a^3/\mu_\bullet}$ is the orbital period, in yr ($\mu_\bullet \doteq GM_\bullet$ is the SMBH’s gravitational parameter given by the product of its mass $M_\bullet = (4.1 \pm 0.2) \times 10^6 M_\odot$ and the Newtonian gravitational constant G), e is the eccentricity, I is the inclination of the orbital plane to the plane of the sky, chosen as reference $\{x, y\}$ plane, Ω is the longitude of the ascending node. Both I and Ω are measured in degrees (°), while e is dimensionless.

the post-Newtonian (pN) static part of the spacetime of the SMBH assumed as nonrotating, are often dubbed in the literature as “gravitoelectric” (Thorne, MacDonald & Price 1986; Mashhoon 2001), in (formal) analogy with the Coulombian electrostatic field of a point charge.

Peißker et al. (2020) explored the possibility of using some of the recently discovered fast-revolving S-stars to measure a peculiar dynamical feature predicted by general relativity as well: the gravitomagnetic Lense–Thirring (LT) orbital precessions induced by the proper angular momentum \mathbf{J} of the central body (Lense & Thirring 1918; Soffel & Han 2019) which, in the present case, is the SMBH in Sgr A*. They arise from the pN stationary, “gravitomagnetic” (Thorne, MacDonald & Price 1986; Thorne 1986, 1988; Mashhoon 2001; Rindler 2001) component of the gravitational field induced by the mass–energy currents which, for an isolated spinning mass, determine just \mathbf{J} . For other gravitomagnetic effects, see, e.g., Dymnikova (1986); Ruggiero & Tartaglia (2002); Schäfer (2004, 2009), and references therein. According to the no-hair theorems (Geroch 1970; Hansen 1974), the magnitude of the angular momentum of a rotating Kerr BH is (Bardeen, Press & Teukolsky 1972; Melia et al. 2001) $J_\bullet = \chi_g M_\bullet^2 G/c$, where $0 \leq \chi_g \leq 1$.

It is not the first time that the idea of looking at the S-stars to perform such a measurement was put forth in the literature (Jaroszynski 1998; Levin & Beloborodov 2003; Kraniotis 2007; Gillessen et al. 2008; Will 2008; Preto & Saha 2009; Angélil, Saha & Merritt 2010; Merritt et al. 2010; Iorio 2011; Merritt 2013; Han 2014; Zhang, Lu & Yu 2015; Psaltis, Wex & Kramer 2016; Yu, Zhang & Lu 2016; Zhang & Iorio 2017; Waisberg et al. 2018; Psaltis 2019). Quite recently, Fragione & Loeb (2020) used the newly discovered S-stars which are the subject of this study to infer upper bounds on χ_g . The main issue with the analysis by Peißker et al. (2020) is that they looked solely at the node precession $\dot{\Omega}^{\text{LT}}$ by means of a formula which holds only in a particular coordinate system whose reference z axis is aligned with the SMBH’s spin axis. Actually, the

orientation in the space of the unit vector $\hat{\mathbf{J}}_\bullet$ of Sgr A* is not known a priori, being, currently, a lingering uncertainty on it. Moreover, for an arbitrary orientation of the primary's spin axis in space, it turns out that also the orbital inclination I and the argument of pericenter ω undergo secular LT precessions. Finally, it is important to remark that \dot{I}^{LT} , $\dot{\Omega}^{\text{LT}}$, and $\dot{\omega}^{\text{LT}}$ depend explicitly on the direction of $\hat{\mathbf{J}}$ in space. Thus, the validity of the figures quoted in Table 3 of Peißker et al. (2020) for $\dot{\Omega}^{\text{LT}}$ is limited since they hold only for the particular case in which the SMBH's spin axis is aligned with the line of sight, assumed as a reference z axis, which, in general, may not be the case. The same drawbacks are common also to Fragione & Loeb (2020). For performed attempts to somehow constrain $\hat{\mathbf{J}}_\bullet$ of Sgr A* with different nondynamical approaches, see Falanga et al. (2007); Meyer et al. (2007); Broderick et al. (2009, 2011); Shcherbakov, Penna & McKinney (2012); Yu, Zhang & Lu (2016), and references therein; it can be seen that the polar angles i^\bullet , ε^\bullet determining the orientation of $\hat{\mathbf{J}}_\bullet$ in space are, in fact, still poorly constrained. In any case, it seems that it is far from being aligned with the line of sight. Indeed, according to, e.g., Meyer et al. (2007), who used polarimetric observations of the near-infrared emission of Sgr A*, it is $i^\bullet \simeq 55^\circ$. Falanga et al. (2007) obtained $i^\bullet \simeq 77^\circ$ on the basis of their fit of a simulated Rossby wave-induced spiral pattern in the SMBH's accretion disk to the X-ray lightcurve detected with XMM-Newton. Shcherbakov, Penna & McKinney (2012) yielded the range $42^\circ \lesssim i^\bullet \lesssim 75^\circ$ by comparing polarized submillimeter infrared observations with spectra computed using three-dimensional general relativistic magnetohydrodynamical simulations. Methods based on gravitational lensing for determining the SMBH's spin direction independently of orbital dynamics were outlined, e.g., in Saida (2017). Takahashi (2004) investigated the possibility of measuring, among other things, i^\bullet from the shape and position of the BH's shadow under certain assumptions.

Here, we make a step forward by providing explicit analytical expressions for the LT precessions of I , Ω , and ω in terms of i , ε . Furthermore, moving to the Sgr A* scenario, we plot them as functions of i^\bullet , ε^\bullet for some selected S-stars among those taken into account by Peißker et al. (2020) by calculating also the values i_0^\bullet , ε_0^\bullet for which the LT precessions vanish along with those, i_{max}^\bullet , $\varepsilon_{\text{max}}^\bullet$ and i_{min}^\bullet , $\varepsilon_{\text{min}}^\bullet$, yielding their maxima and the minima. We look also at the systematic uncertainty affecting the Schwarzschild perinigricon precessions of the considered S-stars due to the errors in the key physical and orbital parameters entering Equation (1). Indeed, this represents a major source of systematic uncertainty in the much smaller LT perinigricon precessions.

2. The Lense–Thirring Orbital Precessions for an Arbitrary Orientation of the SMBH's Spin in Space

The LT orbital precessions for an arbitrary orientation of the angular momentum of the primary in space were worked out in the literature with a variety of analytical techniques encompassing different parameterizations for both the test particle's orbit and the spin itself (see, e.g., Barker & O'Connell 1975; Damour & Schafer 1988; Damour & Taylor 1992; Wex & Kopeikin 1999; Kraniotis 2007; Will 2008; Iorio 2017). According to Iorio (2017), the

gravitomagnetic precessions of the inclination, the node and the periastron are

$$\dot{I} = \frac{2 G J \hat{\mathbf{J}} \cdot \hat{\mathbf{l}}}{c^2 a^3 (1 - e^2)^{3/2}}, \quad (2)$$

$$\dot{\Omega} = \frac{2 G J \csc I \hat{\mathbf{J}} \cdot \hat{\mathbf{m}}}{c^2 a^3 (1 - e^2)^{3/2}}, \quad (3)$$

$$\dot{\omega} = \frac{2 G J \hat{\mathbf{J}} \cdot (2 \hat{\mathbf{h}} + \cot I \hat{\mathbf{m}})}{c^2 a^3 (1 - e^2)^{3/2}}, \quad (4)$$

where $\hat{\mathbf{l}} = \{\cos \Omega, \sin \Omega, 0\}$ is the unit vector directed in the reference $\{x, y\}$ plane along the line of the nodes toward the ascending node, $\hat{\mathbf{m}} = \{-\cos I \sin \Omega, \cos I \cos \Omega, \sin I\}$ is the unit vector directed in the orbital plane transversely to $\hat{\mathbf{l}}$, and $\hat{\mathbf{h}} = \{\sin I \sin \Omega, -\sin I \cos \Omega, \cos I\}$ is the unit vector directed along the orbital angular momentum perpendicularly to the orbital plane in such a way that $\hat{\mathbf{l}}, \hat{\mathbf{m}}, \hat{\mathbf{h}}$ are a right-handed triad of unit vectors. By adopting for $\hat{\mathbf{J}}$ the following parameterization

$$\hat{J}_x = \sin i \cos \varepsilon, \quad (5)$$

$$\hat{J}_y = \sin i \sin \varepsilon, \quad (6)$$

$$\hat{J}_z = \cos i, \quad (7)$$

Equations (2)-(4) can be cast into the form

$$\dot{I}^{\text{LT}} = \frac{2 G J \sin i \cos \zeta}{c^2 a^3 (1 - e^2)^{3/2}}, \quad (8)$$

$$\dot{\Omega}^{\text{LT}} = \frac{2 G J (\cos i + \cot I \sin i \sin \zeta)}{c^2 a^3 (1 - e^2)^{3/2}}, \quad (9)$$

$$\dot{\omega}^{\text{LT}} = -\frac{G J [-6 \cos I \cos i + (1 - 3 \cos 2I) \csc I \sin i \sin \zeta]}{c^2 a^3 (1 - e^2)^{3/2}}. \quad (10)$$

They show that the LT precessions depend explicitly on the absolute orientation of the primary's spin axis and of the test particle's orbital plane in space through i and I , respectively, and on the relative orientation of the primary's spin axis and the test particle's orbit through the angle $\zeta \doteq \varepsilon - \Omega$. As such, they can even vanish for given combinations of i , I , and ζ .

In the case of the S-stars orbiting Sgr A*, Figures 1-3, produced by assuming $\chi_g = 0.5$, $M_\bullet = 4.1 \times 10^6 M_\odot$ (Peißker et al. 2020), depict the plots of $\dot{I}^{\text{LT}}(i^\bullet, \varepsilon^\bullet)$, $\dot{\Omega}^{\text{LT}}(i^\bullet, \varepsilon^\bullet)$, and $\dot{\omega}^{\text{LT}}(i^\bullet, \varepsilon^\bullet)$, in arcseconds per year ($'' \text{ yr}^{-1}$), for S4714, S62, and S4711 whose relevant orbital parameters are listed in Table 1. It can be noted that, for certain values of i^\bullet , ε^\bullet , they vanish, possibly being both positive and negative values.

Tables 2-4 display the values i_0^\bullet , ε_0^\bullet for which the LT precessions vanish, and those corresponding to their minima and maxima. The largest effects occur for the perinigricon

Table 2: Maximum and Minimum Nominal Values, in Arcseconds per Year, of the LT Rate of Change of the Inclination I of Some Selected Short-period S-stars (Peißker et al. 2020) Along with the Corresponding Values, in Degrees, of the SMBH’s Spin Axis Polar Angles $0^\circ \leq i^\bullet \leq 180^\circ$, $0^\circ \leq \varepsilon^\bullet \leq 360^\circ$.

	$\dot{I}_{\text{max}}^{\text{LT}}$ ($'' \text{ yr}^{-1}$)	i_{max}^\bullet ($^\circ$)	$\varepsilon_{\text{max}}^\bullet$ ($^\circ$)	$\dot{I}_{\text{min}}^{\text{LT}}$ ($'' \text{ yr}^{-1}$)	i_{min}^\bullet ($^\circ$)	$\varepsilon_{\text{min}}^\bullet$ ($^\circ$)
S4714	7.04	90	129.3	−7.04	90	309.3
S62	5.15	90	122.6	−5.15	90	302.6
S4711	0.34	90	20.1	−0.34	90	200.1

Note. For $J_\bullet = \chi_g M_\bullet^2 G/c$, the values $\chi_g = 0.5$, $M_\bullet = 4.1 \times 10^6 M_\odot$ (Peißker et al. 2020) were adopted. According to Equation (8), $\dot{I}^{\text{LT}} = 0^\circ$ for the spin axis aligned with the direction of the line of sight, i.e. for $i_0^\bullet = 0^\circ$ or $i_0^\bullet = 180^\circ$, or for $\varepsilon_0^\bullet = \Omega \pm 90^\circ$.

Table 3: Maximum and Minimum Values, in Arcseconds per Year, of the LT Rate of Change of the Node Ω of Some Selected Short-period S-stars (Peißker et al. 2020) Along with the Corresponding Values, in Degrees, of the SMBH’s Spin Axis Polar Angles $0^\circ \leq i^\bullet \leq 180^\circ$, $0^\circ \leq \varepsilon^\bullet \leq 360^\circ$.

	$\dot{\Omega}_{\text{max}}^{\text{LT}}$ ($'' \text{ yr}^{-1}$)	i_{max}^\bullet ($^\circ$)	$\varepsilon_{\text{max}}^\bullet$ ($^\circ$)	$\dot{\Omega}_{\text{min}}^{\text{LT}}$ ($'' \text{ yr}^{-1}$)	i_{min}^\bullet ($^\circ$)	$\varepsilon_{\text{min}}^\bullet$ ($^\circ$)	i_0^\bullet ($^\circ$)	ε_0^\bullet ($^\circ$)
S4714	8.9	37.7	39.3	−8.9	142.3	219.3	77.9	293.3
S62	5.15	0	32.7	−5.32	165.3	360	96.0	142.4
S4711	0.35	8.9	0	−0.34	180	359.9	105.5	237.3

Note. For $J_\bullet = \chi_g M_\bullet^2 G/c$, the values $\chi_g = 0.5$, $M_\bullet = 4.1 \times 10^6 M_\odot$ (Peißker et al. 2020) were adopted. The values i_0^\bullet , ε_0^\bullet yield $\dot{\Omega}^{\text{LT}} = 0^\circ$.

ω , while the smallest ones are those of the inclination I . The star S4714 exhibits the most relevant gravitomagnetic precessions ranging from $14'' \text{ yr}^{-1}$ for ω to $7'' \text{ yr}^{-1}$ for I , while

Table 4: Maximum and Minimum Values, in Arcseconds per Year, of the LT Rate of Change of the Perinigricon ω of Some Selected Short-period S-stars (Peißker et al. 2020) Along with the Corresponding Values, in Degrees, of the SMBH’s Spin Axis Polar Angles $0^\circ \leq i^\bullet \leq 180^\circ$, $0^\circ \leq \varepsilon^\bullet \leq 360^\circ$.

	$\dot{\omega}_{\max}^{\text{LT}}$ ($'' \text{ yr}^{-1}$)	i_{\max}^\bullet ($^\circ$)	$\varepsilon_{\max}^\bullet$ ($^\circ$)	$\dot{\omega}_{\min}^{\text{LT}}$ ($'' \text{ yr}^{-1}$)	i_{\min}^\bullet ($^\circ$)	$\varepsilon_{\min}^\bullet$ ($^\circ$)	i_0^\bullet ($^\circ$)	ε_0^\bullet ($^\circ$)
S4714	14.2	154.9	360	−12.9	0	39.3	102.5	150.7
S62	10.4	63.9	32.6	−10.4	116.0	212.6	55.7	283.1
S4711	0.70	127.6	290.1	−0.70	52.3	110.1	134.2	68.8

Note. For $J_\bullet = \chi_g M_\bullet^2 G/c$, the values $\chi_g = 0.5$, $M_\bullet = 4.1 \times 10^6 M_\odot$ (Peißker et al. 2020) were adopted. The values $i_0^\bullet, \varepsilon_0^\bullet$ yield $\dot{\omega}^{\text{LT}} = 0^\circ$.

those for S4711 are at the subarcsecond per year level. It should be noted that, in general, $i_0^\bullet, \varepsilon_0^\bullet, i_{\max}^\bullet, \varepsilon_{\max}^\bullet, i_{\min}^\bullet, \varepsilon_{\min}^\bullet$ are different from one precession to another for each star.

The fact that the inclination I and the node Ω also exhibit LT precession is, in principle, quite important since using only the perinigricon ω may be an issue because of the uncertainties plaguing its larger Schwarzschild-like rate of change of Equation (1). The propagation of the errors in a , e , and μ_\bullet , listed in Table 1, yield the mismodeling quoted in Table 5. It turns out that

Table 5: Nominal Schwarzschild Perinigricon Precessions $\dot{\omega}^{\text{Sch}}$, in Arcseconds per Year, of the S-stars S4714, S62, S4711 and Related Uncertainties $\delta\dot{\omega}_{\sigma_x}^{\text{Sch}}$, in Arcseconds per Year, Due to the Errors in $x = a, e, \mu_\bullet$. According to Table 1.

	$\dot{\omega}^{\text{Sch}}$ ($'' \text{ yr}^{-1}$)	$\delta\dot{\omega}_{\sigma_a}^{\text{Sch}}$ ($'' \text{ yr}^{-1}$)	$\delta\dot{\omega}_{\sigma_e}^{\text{Sch}}$ ($'' \text{ yr}^{-1}$)	$\delta\dot{\omega}_{\sigma_{\mu_\bullet}}^{\text{Sch}}$ ($'' \text{ yr}^{-1}$)
S4714	521.1	3.8	379.2	38.1
S62	450.8	6.3	185.6	33.0
S4711	81.4	4.0	9.1	5.9

the main source of systematic bias is the eccentricity e ; the corresponding mismodeled parts of $\dot{\omega}^{\text{Sch}}$ largely overwhelm the LT precessions for all the S-stars considered. Also, the mass of the SMBH should be known with a much better accuracy since its uncertainty yields systematic errors in $\dot{\omega}^{\text{Sch}}$ larger than $\dot{\omega}^{\text{LT}}$. Instead, I and Ω do not undergo huge competing Schwarzschild precessions.

In principle, also other competing dynamical effects may bias a potential detection of the

LT orbital precessions because of their mismodeling or unmodeling. One of them, generally impacting I , Ω , ω , is the Newtonian 3-body perturbation on the target S-star induced by other distant stars for which analytical expressions exist in the literature either for their double average over both P_b and the longer orbital period of the perturber as well; see, e.g., Iorio (2020). The assessment of the systematic uncertainties in the LT measurement depends on the mismodeling in the mass m of the third body and in its orbital parameters. Another orbital perturbation to be taken into account, in principle, is that caused by a possible continuous mass distribution, baryonic or not, inside the orbit of the S-star of interest. If its density ϱ is spherically symmetric, it affects only the perinigricon ω (Iorio 2013). Dedicated analyses, including, e.g., simultaneous numerical integrations of the equations of motion of given target stars and other disturbing ones for different values of the masses of the latter are required; they are beyond the scope of the present paper.

3. Summary and conclusions

In principle, the inclination I , the longitude of the ascending node Ω and the argument of perinigricon ω of some of the recently discovered fast-revolving S-stars can be used to measure their gravitomagnetic LT effect induced by the angular momentum J_\bullet of the SMBH in the GC at Sgr A*. Such general relativistic orbital precessions depend explicitly on the orientation of \hat{J}_\bullet in space, and in general, are all nonzero. Indeed, present-day constraints on its polar angles i^\bullet , ε^\bullet , despite being still rather weak, are accurate enough to exclude that the SMBH's spin is aligned with the line of sight; thus, also \dot{I}^{LT} which is proportional to $\sin i^\bullet$, is likely nonzero. We calculated the maxima and minima for \dot{I}^{LT} , $\dot{\Omega}^{\text{LT}}$, $\dot{\omega}^{\text{LT}}$ along with the corresponding values i_{max}^\bullet , $\varepsilon_{\text{max}}^\bullet$ and i_{min}^\bullet , $\varepsilon_{\text{min}}^\bullet$ for each star. We obtained $|\dot{I}^{\text{LT}}| \lesssim 7'' \text{ yr}^{-1}$, $|\dot{\Omega}^{\text{LT}}| \lesssim 9'' \text{ yr}^{-1}$, and $-13'' \text{ yr}^{-1} \lesssim \dot{\omega}^{\text{LT}} \lesssim 14'' \text{ yr}^{-1}$ for S4714, $|\dot{I}^{\text{LT}}| \lesssim 5'' \text{ yr}^{-1}$, $|\dot{\Omega}^{\text{LT}}| \lesssim 5'' \text{ yr}^{-1}$, and $|\dot{\omega}^{\text{LT}}| \lesssim 10'' \text{ yr}^{-1}$ for S62, and $|\dot{I}^{\text{LT}}| \lesssim 0.3'' \text{ yr}^{-1}$, $|\dot{\Omega}^{\text{LT}}| \lesssim 0.3'' \text{ yr}^{-1}$, and $|\dot{\omega}^{\text{LT}}| \lesssim 0.7'' \text{ yr}^{-1}$ for S4711. We also determined the values i_0^\bullet , ε_0^\bullet for which the LT precessions vanish.

Despite the largest values occurring for the arguments of perinigricon ω of S4714 and S62, being at the level of $\simeq 10'' \text{ yr}^{-1}$, the use of such orbital elements is made problematic by the systematic bias arising from the mismodeling in their much larger Schwarzschild precessions due to the current errors in the stellar orbital elements, especially in the eccentricity e , and the mass of Sgr A* itself. Suffice to say that while the nominal gravitoelectric 1pN rates are $\dot{\omega}^{\text{Sch}} = 521'' \text{ yr}^{-1}$ (S4714) and $\dot{\omega}^{\text{Sch}} = 451'' \text{ yr}^{-1}$ (S62), the mismodeling due to the current errors in e are as large as $\delta\dot{\omega}_{\sigma_e}^{\text{Sch}} = 379'' \text{ yr}^{-1}$ and $\delta\dot{\omega}_{\sigma_e}^{\text{Sch}} = 185'' \text{ yr}^{-1}$, respectively, while those due to the SMBH's mass uncertainty amount to $\delta\dot{\omega}_{\sigma_{\mu_\bullet}}^{\text{Sch}} = 38'' \text{ yr}^{-1}$ and $\delta\dot{\omega}_{\sigma_{\mu_\bullet}}^{\text{Sch}} = 33'' \text{ yr}^{-1}$, respectively.

Other potentially relevant sources of systematic errors, to be analyzed in further dedicated studies, are the classical competing orbital precessions due to other distant stars acting as pointlike disturbing bodies affecting, in general, I , Ω , and ω , and to possible continuous mass distribution, baryonic or not, around the SMBH which, if spherically symmetric, perturbs only the perinigricon.

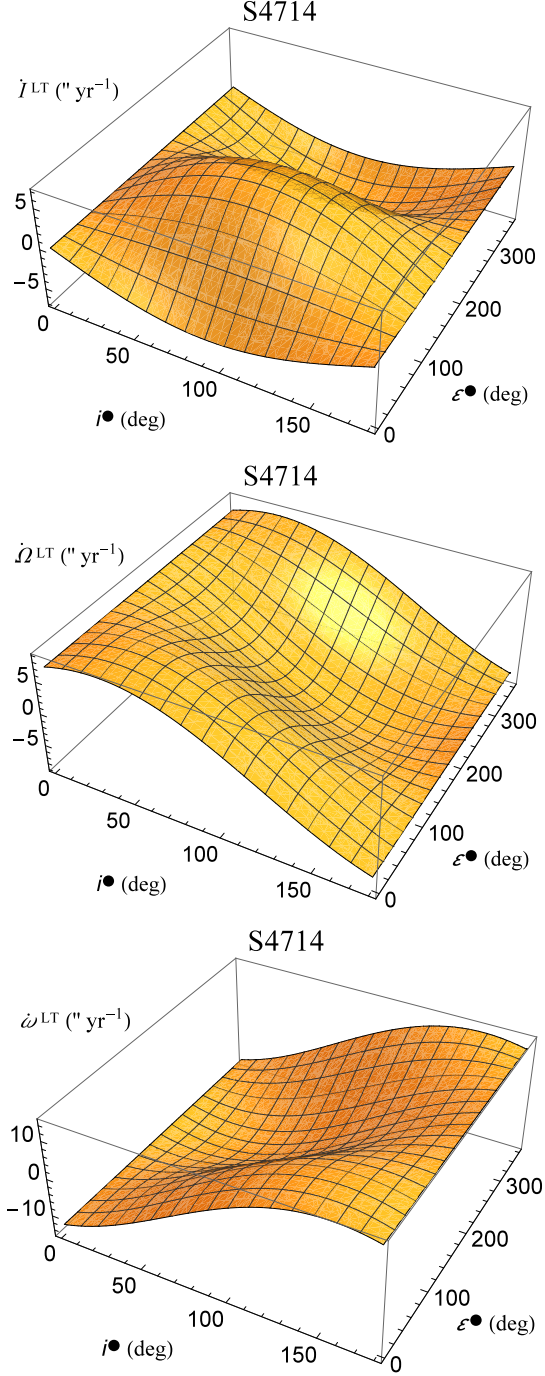


Fig. 1.— LT precessions, in arcseconds per year, of the S-star S4714 according to Equations (8)-(9) plotted as functions of i^\bullet , ϵ^\bullet . For $J_\bullet = \chi_g M_\bullet^2 G/c$, the values $\chi_g = 0.5$, $M_\bullet = 4.1 \times 10^6 M_\odot$ (Peißker et al. 2020) were adopted.

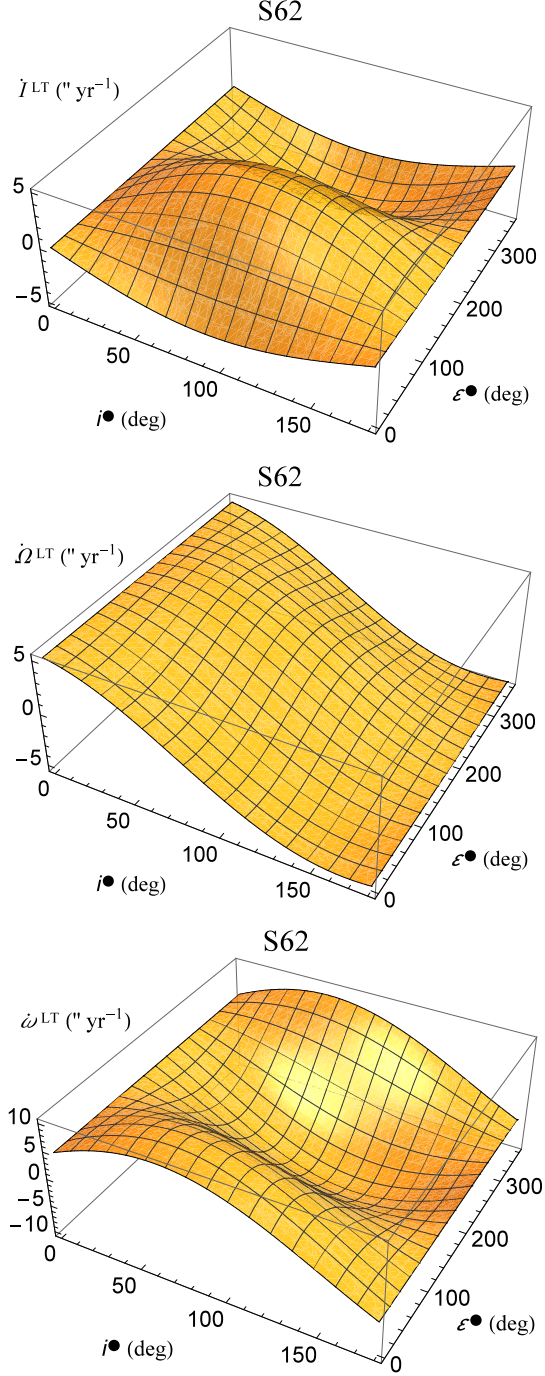


Fig. 2.— LT precessions, in arcseconds per year, of the S-star S62 according to Equations (8)-(9) plotted as functions of i^\bullet , ϵ^\bullet . For $J_\bullet = \chi_g M_\bullet^2 G/c$, the values $\chi_g = 0.5$, $M_\bullet = 4.1 \times 10^6 M_\odot$ (Peißker et al. 2020) were adopted.

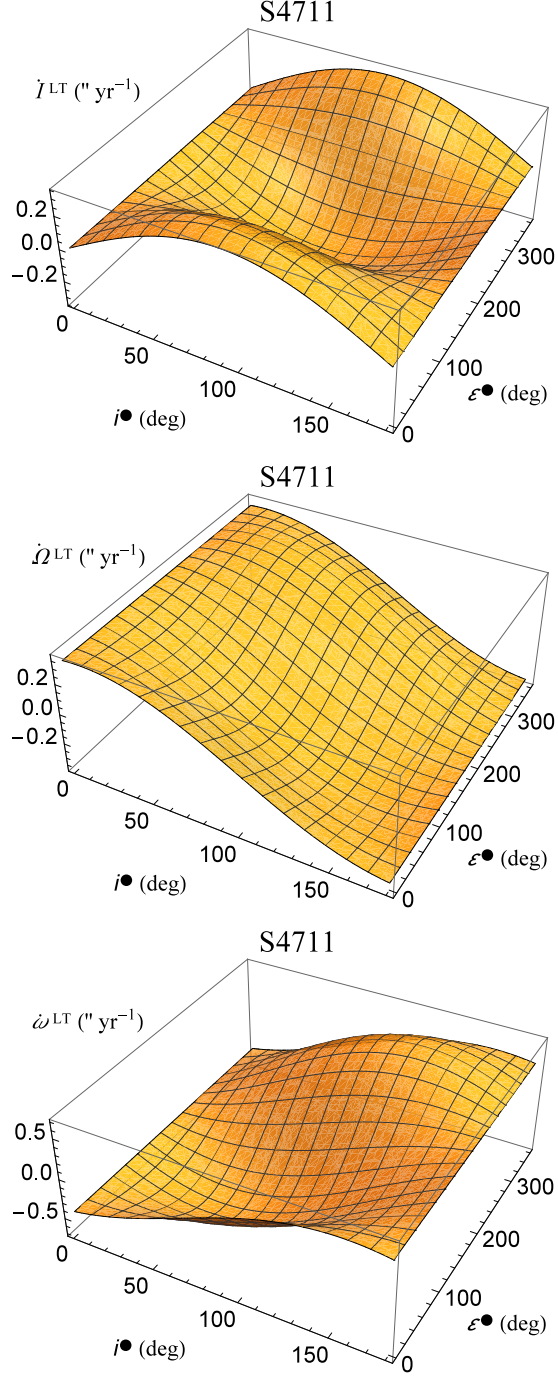


Fig. 3.— LT precessions, in arcseconds per year, of the S-star S4711 according to Equations (8)-(9) plotted as functions of i_\bullet , ϵ_\bullet . For $J_\bullet = \chi_g M_\bullet^2 G/c$, the values $\chi_g = 0.5$, $M_\bullet = 4.1 \times 10^6 M_\odot$ (Peißker et al. 2020) were adopted.

REFERENCES

- Angélil R., Saha P., Merritt D., 2010, *ApJ*, 720, 1303
- Bardeen J. M., Press W. H., Teukolsky S. A., 1972, *ApJ*, 178, 347
- Barker B. M., O’Connell R. F., 1975, *PhRvD*, 12, 329
- Broderick A. E., Fish V. L., Doeleman S. S., Loeb A., 2009, *ApJ*, 697, 45
- Broderick A. E., Fish V. L., Doeleman S. S., Loeb A., 2011, *ApJ*, 735, 110
- Damour T., Schafer G., 1988, *NCimB*, 101, 127
- Damour T., Taylor J. H., 1992, *PhRvD*, 45, 1840
- Dymnikova I. G., 1986, *SvPhU*, 29, 215
- Falanga M., Melia F., Tagger M., Goldwurm A., Bélanger G., 2007, *ApJL*, 662, L15
- Fragione G., Loeb A., 2020, *ApJL*, 901, L32
- Genzel R., Eisenhauer F., Gillessen S., 2010, *RvMP*, 82, 3121
- Geroch R., 1970, *JMP*, 11, 2580
- Ghez A. M. et al., 2008, *ApJ*, 689, 1044
- Gillessen S., Genzel R., Eisenhauer F., Ott T., Trippe S., Martins F., 2008, in *IAU Symposium*, Vol. 248, *A Giant Step: from Milli- to Micro-arcsecond Astrometry*, Jin W. J., Platais I., Perryman M. A. C., eds., pp. 466–469
- Gillessen S. et al., 2017, *ApJ*, 837, 30
- Gravity Collaboration et al., 2018, *A&A*, 615, L15
- Gravity Collaboration et al., 2020, *A&A*, 636, L5
- Han W.-B., 2014, *RAA*, 14, 1415
- Hansen R. O., 1974, *JMP*, 15, 46
- Iorio L., 2011, *MNRAS*, 411, 453
- Iorio L., 2013, *Galax*, 1, 6
- Iorio L., 2017, *EPJC*, 77, 439
- Iorio L., 2020, *ApJ*, 889, 152

- Jaroszynski M., 1998, *AcA*, 48, 653
- Kraniotis G. V., 2007, *CQGra*, 24, 1775
- Lense J., Thirring H., 1918, *PhyZ*, 19, 156
- Levin Y., Beloborodov A. M., 2003, *ApJL*, 590, L33
- Martins F., Gillessen S., Eisenhauer F., Genzel R., Ott T., Trippe S., 2008, *ApJL*, 672, L119
- Mashhoon B., 2001, in *Reference Frames and Gravitomagnetism*, Pascual-Sánchez J. F., Floría L., San Miguel A., Vicente F., eds., pp. 121–132
- Melia F., Bromley B. C., Liu S., Walker C. K., 2001, *ApJL*, 554, L37
- Merritt D., 2013, *Dynamics and Evolution of Galactic Nuclei*. Princeton University Press, Princeton
- Merritt D., Alexander T., Mikkola S., Will C. M., 2010, *PhRvD*, 81, 062002
- Meyer L., Schödel R., Eckart A., Duschl W. J., Karas V., Dovčiak M., 2007, *A&A*, 473, 707
- Peißker F., Eckart A., Zajaček M., Ali B., Parsa M., 2020, *ApJ*, 899, 50
- Preto M., Saha P., 2009, *ApJ*, 703, 1743
- Psaltis D., 2019, *GReGr*, 51, 137
- Psaltis D., Wex N., Kramer M., 2016, *ApJ*, 818, 121
- Rindler W., 2001, *Relativity: special, general, and cosmological*. Oxford University Press, Oxford, UK
- Ruggiero M. L., Tartaglia A., 2002, *NCimB*, 117, 743
- Saida H., 2017, *PTEP*, 2017, 053E02
- Schäfer G., 2004, *GReGr*, 36, 2223
- Schäfer G., 2009, *SSRv*, 148, 37
- Shcherbakov R. V., Penna R. F., McKinney J. C., 2012, *ApJ*, 755, 133
- Soffel M. H., Han W.-B., 2019, *Applied General Relativity, Astronomy and Astrophysics Library*. Springer Nature Switzerland, Cham
- Takahashi R., 2004, *ApJ*, 611, 996

- Thorne K. S., 1986, in *Highlights of Modern Astrophysics: Concepts and Controversies*, Shapiro S. L., Teukolsky S. A., Salpeter E. E., eds., Wiley, NY, p. 103
- Thorne K. S., 1988, in *Near Zero: New Frontiers of Physics*, Fairbank J. D., Deaver Jr. B. S., Everitt C. W. F., Michelson P. F., eds., W. H. Freeman, New York, pp. 573–586
- Thorne K. S., MacDonald D. A., Price R. H., eds., 1986, *Black Holes: The Membrane Paradigm*. Yale University Press, Yale
- Waisberg I. et al., 2018, *MNRAS*, 476, 3600
- Wex N., Kopeikin S. M., 1999, *ApJ*, 514, 388
- Will C. M., 2008, *ApJL*, 674, L25
- Yu Q., Zhang F., Lu Y., 2016, *ApJ*, 827, 114
- Zhang F., Iorio L., 2017, *ApJ*, 834, 198
- Zhang F., Lu Y., Yu Q., 2015, *ApJ*, 809, 127